Electrochemical Formation of Luminescent Convective Patterns in Thin-Layer Cells

Marek Orlik,† Jürgen Rosenmund, Karl Doblhofer,* and Gerhard Ertl

Fritz-Haber-Institut der Max-Planck-Gesellschaft, Faradayweg 4-6, D-14195 Berlin, Germany

Received: June 11, 1997; In Final Form: December 3, 1997

The electrolysis of rubrene in a thin-layer electrochemical cell leads to formation of electrohydrodynamic (EHD) convection patterns. The well-known electrochemiluminescence produced in this process renders the convective structures clearly visible. The electrochemical mechanism leading to the EHD convection is analyzed. In particular, the importance of ionic salt concentration is elucidated. Example structures are shown, and the basic mechanism of their formation by convective flows is proposed.

1. Introduction

Investigations of the principles that lead to self-organization of previously homogeneous matter have become a subject of great interest.[1−4] Such knowledge constitutes a basis for a better understanding of processes in living systems; it may also provide completely new ways for controlling technical processes.

The subject of this work is hydrodynamic instabilities, leading to convective patterns.[2−10] In liquids subject to thermal convection, realized in a thin layer of fluid exposed to a temperature gradient, convective hexagonal cells (resembling honeycombs), as reported first by Bénard,[5] or rolls with different degrees of complexity[2−4,6,10] can be observed. The basic cause for these classical Rayleigh instabilities[7,8] is density gradients of the fluid. Such density gradients can result also under isothermal conditions from concentration gradients in a solution, e.g., during electrolysis between two electrodes.[4,11−15] With a free fluid surface Marangoni instabilities,[3,4] involving gradients of a surface tension, may interfere with Rayleigh instabilities. Under certain conditions, these instabilities can even give rise to chaotic patterns.[3]

Electrohydrodynamic (EHD) *convection* is observed in charged fluids under the influence of an electrical field.[16−31] The driving force of such convection, sometimes called the Felici instability,[30,31] is the interaction of the electric field with an uncompensated *space charge* which can be transported by the moving fluid. An example of electrohydrodynamic convection are patterns of instabilities (e.g., Williams domains) observed in thin layers of nematic liquid crystals exposed to dc or ac field.[32−36] An interplay of electrical and photochemical phenomena leads to patterns of *photoelectrohydrodynamic* convection.[37]

A particularly remarkable variant of an EHD convection experiment has been described by Schaper, Schnedler, and Köstlin.[21−25] A constant voltage was applied across a thin-layer (10−100 μm) electrochemical cell containing a solution of rubrene (5,6,11,12-tetraphenylnaphthacene) in 1,2-dimethoxyethane (1,2-DME). The electrolysis of rubrene produces charged radicals migrating in the electrical field ($\sim 10^3$ V cm^{-1}). As the reaction between cationic and anionic radicals of rubrene leads to chemiluminescence,[38,39] the evolution of convective structures can be visualized as pattern of bright luminescence. Quasi-hexagonal arrangements of spots, resembling Bénard structures, were reported. Later Jaguiro, Smirnov, and Zhivnov[26−29] continued these studies. A simple model of observed motions was proposed,[26] and possible practical applications of the luminescent EHD in liquid pumps, dynamic light scattering, and electrochemiluminescence displays[26,27] were suggested.

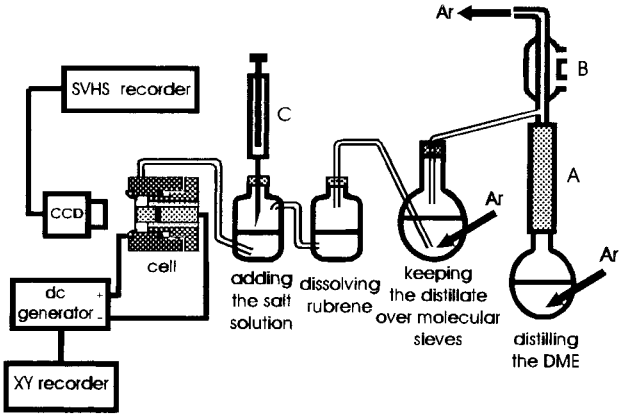

Figure 1. Scheme of the laboratory equipment for observing convective structures of electrochemiluminescence of rubrene in a thin-layer electrochemical cell: A, Vigreux column; B, cooler; C, microsyringe.

Luminescent EHD patterns can be studied more thoroughly with the modern tools of image recording and processing. It is considered that such studies will lead to new valuable insight into the underlying electrochemical processes and the complex nonlinear dynamics. In particular, it appears important to elucidate the role of ionic contaminants[21−24] or pretreatment of the cell with relatively high voltage (up to 50 V),[40] which have been suggested as a precondition for formation of the EHD structures. In this paper we present the results of such studies, the particular aim of which was: (i) to analyze the state of the system that leads to the electroconvective motion of liquid and (ii) to describe the basic geometrical features of luminescent patterns.

2. Experimental Section

The experimental setup is sketched in Figure 1 and was designed to warrant extremely pure reagents. A solution of rubrene in dimethoxyethane (distilled under argon and then kept

* Corresponding author: fax (+ 030) 8413−3101, e-mail doblhofer@fhi-berlin.mpg.de.

† Permanent address: University of Warsaw, Department of Chemistry, ul. Pasteura 1, 02-093 Warsaw, Poland.

S1089-5647(97)01912-3 CCC: $15.00 © 1998 American Chemical Society
Published on Web 01/30/1998

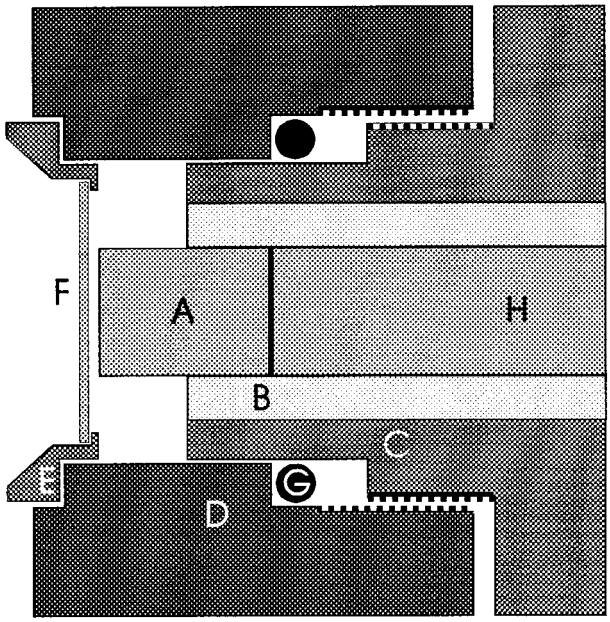

Figure 2. Simplified cross section of the thin-layer electrochemical cell: A, copper (gold, platinum) electrode; B, KEL-F insulating layer; C, metallic (bronze and steel) movable block; D, metallic (bronze) fixed block connected with part C by the thread; E, steel ring for fixing the glass electrode; F, transparent electrode (glass plate coated with ITO); G, sealing O-ring; H, copper rod (for copper electrode A and H denote a single copper rod). For clarity, several O-rings, threads, and supply and outlet lines for the solution and the inert gas (argon) are omitted.

over molecular sieves 4A) is prepared in a closed system under exclusion of oxygen and water. This solution may then be enriched with small amounts of a supporting electrolyte (tetrabutylammonium hexafluorophosphate) and transferred under pressure of argon to the two-electrode electrolytic cell with one electrode metallic (Cu, Au, or Pt) and the one transparent (conducting glass surface). Patterns of luminescence evolved after application of the dc voltage between these electrodes were observed on the monochrome monitor (with about 80 times magnification) connected to the CCD (charge coupled device) camera and recorded on a video tape. For each experiment also the current−voltage characteristics of the system were determined. As the interelectrode distance is an important control factor, it was determined from measurements of the capacitance of the cell, as described below.

As a source of dc voltage, a homemade sweep generator was used. A digital multimeter with an analog signal output (Keithley 177 Microvolt DMM) was used to measure the current. The current−voltage characteristics of the system were recorded by an XY recorder BD 91 (Kipp & Zonen).

The capacitance measurements of the electrochemical cell were performed with a lock-in-amplifier (model 5210, EG&G).

A monochrome CCD camera, Fujitsu model TCZ-230 EA, was used, together with an SVHS video recorder NV-HS1000 EGC (Panasonic), for recording the luminescent patterns on the SVHS-SE-180 video tape (Fuji). The images were digitized with a computerized setup, consisting of a digital video recorder and a Sun workstation.

The construction of the electrochemical cell is shown in Figure 2. It consists of metallic (bronze and steel) blocks, interconnected with a fine thread (500 μm for one full turn, with a division marked every 2°), allowing the precise adjustment of the interelectrode distance. The cylindrical copper rod is isolated from the rest of the cell through a layer of the KEL-F plastic. To the front of that rod gold or platinum electrodes can be fixed. The front circular surface of this electrode was polished flat down to 1 μm.

The transparent electrode was made by coating the glass plates (diameter 3 cm) with an ITO layer (In_2O_3:Sn) of about 200 nm thickness by sputtering.

To avoid the electrochemical decomposition of the copper electrode during the experiments, it was always polarized cathodically with respect to the ITO electrode. Gold and platinum electrodes worked both as a cathode and an anode.

The interelectrode distance d in the electrolytic cell was determined from capacitance measurements:

$$C_{el} = \epsilon\epsilon_0 \frac{A_{met}}{d} = \epsilon\epsilon_0 \frac{A_{met}}{d_{th} + \Delta d} \quad (1)$$

where C_{el} is the capacitance of the system metal electrode−ITO electrode, $A_{met} = 2.011$ cm^2 is the surface area of a metal (Cu, Au, Pt) electrode (smaller than that of the counter electrode, $A = 7.070$ cm^2), ϵ is the relative dielectric constant of the medium, $\epsilon_0 = 8.85419 \times 10^{-12}$ F m^{-1} is the permittivity of a vaccum, and d_{th} is the interelectrode distance read from the characteristics of the thread with an uncertainty (offset) Δd originating from limited mechanical precision of the thread, certain roughness of the electrode surface, and deviations of parallel position of two electrode surfaces. Δd was typically of the order 6−9 μm as derived by adjusting C_{el} to $(d_{th} + \Delta d)^{-1}$ to a linear relationship. For comparison, interelectrode distances were determined from capacity measurements of the cell filled with carbon tetrachloride ($\epsilon = 2.238$ at 20 °C[41]) and led to practically the same results.

The interelectrode distances were checked before each series of experiments.

Commercially available rubrene (for chemiluminescence, Fluka), 1,2-dimethoxyethane (puriss., Fluka, <0.005% H_2O), and tetrabutylammonium hexafluorophosphate (puriss., Fluka) were used. Rubrene and tetrabutylammonium hexafluorophosphate were predried over vacuum at about 80 °C. Dimethoxyethane, commercially packed under argon and kept in contact with molecular sieves, was additionally distilled prior to the experiment in argon atmosphere. The first 10% of a distillate was discarded. The distillate was kept over molecular sieves 4A, first predried at about 400 °C in a vacuum. Commercially available carbon tetrachloride (p.a. Fluka) was used without any further purification.

3. Results

Figure 3a represents a series of current−voltage curves obtained with 1,2-DME solutions saturated with rubrene (~4 × 10^{-3} mol dm^{-3}). In the sequence of curves 1−7 the concentration of added background electrolyte has been increased from zero to approximately 1 × 10^{-4} mol dm^{-3}. Note that, contrary to previous results,[22,23] the electrolyte-free solution of rubrene in dimethoxyethane (curve 1) did not yield any significant currents. Current densities similar to the ones reported in the literature were observed only after addition of small amount (5 × 10^{-6}−2 × 10^{-5} mol dm^{-3}) of background electrolyte−tetrabutylammonium hexafluorophosphate (TBA^+-HFP^-).

There is a hysteresis in the $I-U$ curves with a tendency for the current to increase with time, as demonstrated by Figure 3b for three subsequent measurements, conducted at a concentration of 1.2 × 10^{-5} mol dm^{-3} tetrabutylammonium hexafluorophosphate.

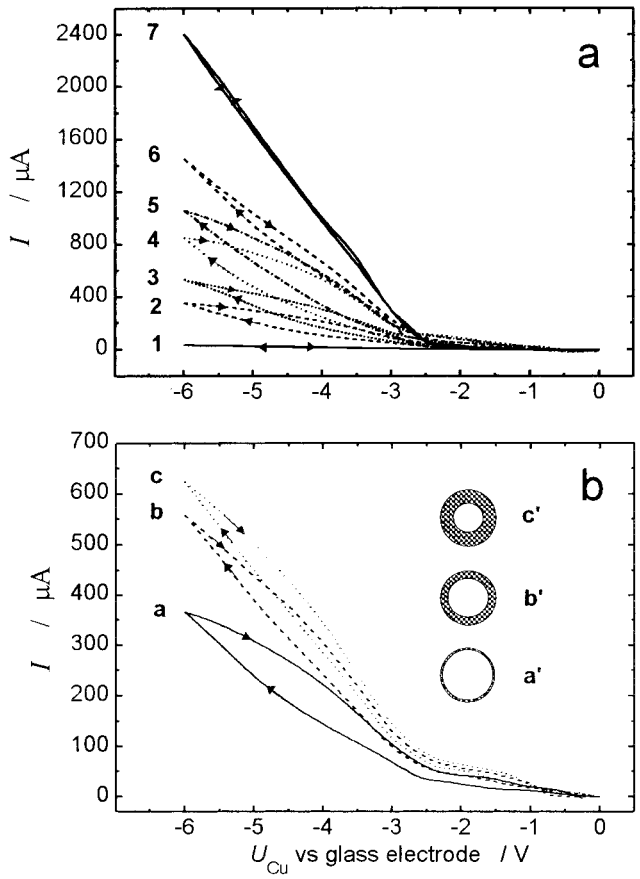

Figure 3. Current−voltage (I/U) characteristics of the electrochemical thin-layer cell ($d = 64$ μm) filled with a saturated solution of rubrene in 1,2-dimethoxyethane, for a potential sweep rate 50 mV s^{-1}. (a) First current−voltage cyclic curve for different concentrations of tetrabutylammonium hexafluorophosphate: (1) 0, (2) 5×10^{-6}, (3) 1×10^{-5}, (4) 2×10^{-5}, (5) 3×10^{-5}, (6) 5.2×10^{-5}, and (7) 9.7×10^{-5} mol dm^{-3}; (b) a−c: three subsequent current−voltage cyclic curves for 1.2×10^{-5} mol dm^{-3} tetrabutylammonium hexafluorophosphate; a′−c′: The luminescent (= shaded) areas of the circular electrode surface observed simultaneously with the I/U curves a−c.

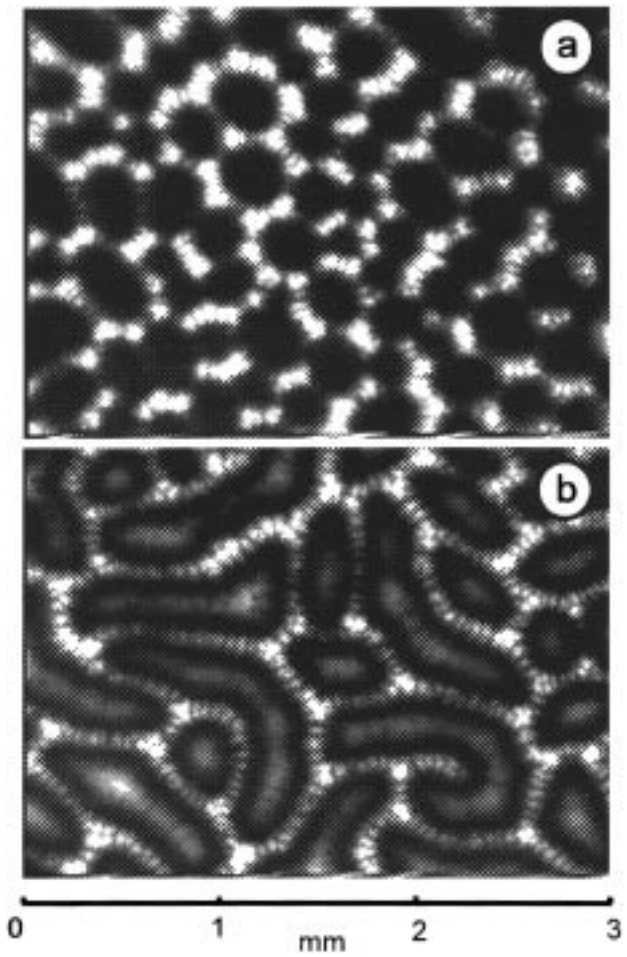

Figure 4. Typical convective patterns of luminescence, observed for the saturated solution of rubrene in 1,2-DME using Cu electrode as the cathode: (a) Cellular (quasi-hexagonal) cathodic structures for 7×10^{-6} mol dm^{-3} tetrabutylammonium hexafluorophosphate, $U = 4.5$ V, interelectrode distance $d = 175$ μm; the mean ratio between the diameter of rounded cells and the interelectrode distance is close to 2 (b) Cathodic−anodic convective structure, for 1.2×10^{-5} mol dm^{-3} tetrabutylammonium hexafluorophosphate, $U = 4$ V and $d = 120$ μm. Bright and sharp luminescence occurred near the cathode surface (Cu) while at the glass anode the weaker and more diffuse luminescence was observed.

In the inset of Figure 3b (pictures a′−c′), the luminescent area of the thin-layer cell (defined by the size and shape of the metal electrode) is sketched. Initially, the strongest luminescence originates from a peripheral ring section (a′). With time, the area of the glowing ring increases toward the interior region of the thin-layer cell (b′, c′). When the concentration of background electrolyte is larger, the luminescent ring is initially larger, and its expansion to the interior part proceeds faster. Furthermore, the interior portion of the cell can be brought into the luminescent state by agitating the solution, in particular by repeated variation of the interelectrode distance (cf. Figure 2). In the following, this activation of the electrode will be termed "conditioning". Such conditioning leads to a state of the system in which the luminescence phenomena can be observed for periods of up to hours. After the conditioning, convective structures develop instantaneously at the entire surface if the voltage is switched on, after the voltage interruption of several seconds.

Enlargement of the area of luminescence is always associated with an increase in current, indicating that luminescence reflects the extent of electrolysis of rubrene and thus the extent of the activation of the electrode surface. Although it is difficult to measure this relationship precisely, it is suggested that, for a given voltage and concentration of background electrolyte, the true current density may be roughly constant for curves reproduced in Figure 3b. For the highest concentration of a supporting electrolyte (curve 7 in Figure 3a) the current, flowing at a voltage 5 V, is close to 2 mA. Since for those experimental conditions almost the whole electrode surface exhibited the bright luminescence and $S_{Cu} \approx 2$ cm^2, the corresponding current density should be close to $j = 1$ mA cm^{-2}.

The current−voltage curves are similar for different metallic electrodes when they are polarized cathodically (Cu, Au, Pt) or anodically (Au, Pt). Also, the distribution of luminescence is similar with the exception that for the cathodically polarized platinum electrode the luminescence appears usually on larger area (including the central part of the electrode).

The luminescence patterns under stable convection conditions are typically in the form of closed (frequently quasi-hexagonal) cells or are of elongated curvilinear shape (resembling fingerprints, boomerangs, etc.), depending on the particular experimental parameters (Figure 4). Cellular patterns (Figure 4a) predominate at higher voltages; their diameter (d_{lum}) is close to or somewhat above the doubled interelectrode distance ($2d$−$2.7d$), as proposed previously.[20,25] Our video recordings show that the velocity of convective flows, i.e., the motion of light-

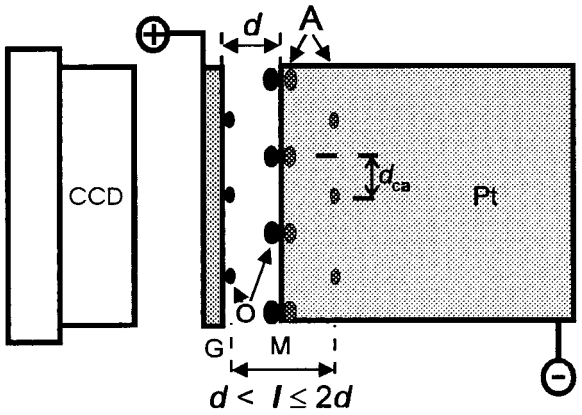

Figure 5. Scheme of experiments establishing the position of luminescence at glass (G) and platinum (Pt) electrodes, using the polished surface of a platinum electrode as a mirror (M). The CCD camera was focused on the original (O) and apparent (A) pictures of convective structures. Example result for 5×10^{-6} mol dm^{-3} tetrabutylammonium hexafluorophosphate and $U = 5.5-7$ V: stronger luminescence is observed at the cathode (Pt), with hardly distinguishable apparent image; the weaker luminescence appears at the anode, with apparent image at $d < l \leq 2d$. The distance between neighboring cathodic and anodic luminescence ($d_{ca.}$) is equal to or slightly higher than the interelectrode distance d.

emitting fluid patches, increases with increasing applied voltage. For typical conditions ($d = 100-200$ μm, $U = 4-6$ V) this velocity is of the order of 1−3 mm s^{-1}. At larger distances ($\geq$200 μm) convection is slower, and the structures frequently reveal slow evolution into vertically elongated rolls, according to the direction of the gravitational field.

With increasing concentration of tetrabutylammonium hexafluorophosphate two effects are observed. First, at the same voltage, for which rounded cells were observed at lower salt concentrations, now more elongated (roll-like) features appear. The distance between the neighboring walls of such rolls is close to the doubled interelectrode distance ($2d$). Second, for higher salt concentrations, in the space between the walls of rolls, areas of new, but usually weaker, luminescence appear (Figure 4b). By focusing the CCD camera on both luminescence traces, we found that their positions in the bulk of the solution are separated by a distance close to, or slightly smaller than, the interelectrode distance d, so that actually both cathodic and anodic luminescence patterns are existing.

The stronger luminescence was found to be located near the cathode. This is in contradiction to previous results suggesting the existence of luminescence only close to the anode surface.[22,23,40] Further confirmation of the presented observations was obtained by experiments, in which the polished surface of a platinum electrode was used as a mirror. In this case the CCD camera could be focused on either the original luminescence or its apparent image (Figure 5).

4. Discussion

The rubrene (Ru) molecules undergo fast (reversible) electroreduction and electrooxidation at the appropriate electrodes, when the electrical double layers are formed:

cathode

$$Ru + e^- \rightarrow Ru^- \quad (2a)$$

$$Ru^+ + 2e^- \rightarrow Ru^- \quad (2b)$$

anode

$$Ru - e^- \rightarrow Ru^+ \quad (3a)$$

$$Ru^- - 2e^- \rightarrow Ru^+ \quad (3b)$$

The recombination reaction

$$Ru^+ + Ru^- \rightarrow Ru^* + Ru \quad (4)$$

leads to rubrene in the excited state (Ru*), which reacts further under light ($h\nu$) emission:[21−29,38,39]

$$Ru^* \rightarrow Ru + h\nu \quad (5)$$

As the voltage is applied to the thin-layer cell, ions from the background electrolyte migrate to the electrodes to form the electrical double layers. At the cathode TBA^+ ions accumulate while HFP^- anions migrate to the anode. For a typical double-layer capacity $C_d = 15$ μF cm^{-2} and a voltage drop inside the double layer $\Delta\phi_{dl} = 1$ V, a surface charge density of 15 μC cm^{-2} results. This corresponds to a surface density 0.15 nmol cm^{-2} of ions of 1:1 electrolyte. The typical concentration of background electrolyte is 10^{-8} mol cm^{-3}, yielding 0.10 nmol cm^{-2} of ions in the solution layer of $d = 100$ μm.

This means that for typical experimental conditions of the thin-layer EHD cell the volume between the electrodes will be largely depleted from the ions of background electrolyte. The buildup of the interfacial potential drops may not reach the values of $\Delta\phi_{dl}$ corresponding to $E°(Ru/Ru^+)$ and $E°(Ru/Ru^-)$ that are required for rubrene oxidation and reduction. The influx of ions from the surrounding electrolyte solution may be necessary. This is the reason for the requirement of "conditioning" described above.

When, after efficient "conditioning", voltage is switched off, double layers are released, and the actual concentration of a supporting electrolyte (c') in the interelectrode space d gets higher than in surroundings (c^0):

$$c' = c^0 + C_d\Delta\varphi_{dl}/FAd \quad (6)$$

When voltage is soon switched on again, the double layers are reconstructed, and the concentration of the interelectrode solution is reduced again to c^0.

It is noteworthy that for typical concentrations of 1:1 supporting electrolyte ($5 \times 10^{-6}-2 \times 10^{-5}$ mol dm^{-3}), as that used by us, the extent of the diffuse part of double layers, estimated as 1.5 times the Debye's length $\kappa^{-1} = [\epsilon\epsilon_0 RT/(2F^2c^0)]^{1/2}$ for 1,2-DME ($\epsilon = 7.2$[42]), is equal to 62−32 nm, respectively. This means that the space occupied by double layers forming in our system is negligibly small in comparison with the entire interelectrode distance d, ranging from 20 to 500 μm.

Thus, the driving force for the electroconvection is determined by the interaction of the electric field with space charge carried by the liquid between the two double layers. This space charge originates from a certain density of uncompensated charge of mobile ions, when the solution is not electroneutral.

Let us first consider the formation of driving force in terms of the model of unipolar charge injection of rubrene ions, as suggested in the literature.[22,23,26] Since the mobility of HFP^- is larger than that of TBA^+ (see below), after application of the voltage the interfacial potential drop $\Delta\phi_{dl}$ at the anode will first reach the value required for the anodic oxidation $Ru \rightarrow Ru^+ + e^-$. Let us assume that the produced Ru^+ ions are transported without charge compensation across the solution

depleted from ions. The expected space-charge-limited current density j_{sclc} is given by[17,31]

$$j_{sclc} = \frac{9}{8}\epsilon\epsilon_0\mu_{Ru^+}\frac{U_{eff}^{\ 2}}{d^3} \quad (7)$$

where μ_{Ru^+} denotes the true (nonconvective) ionic mobility of charge carriers (of rubrene radical cations) in 1,2-DME, and U_{eff} is the effective voltage drop across the solution, resulting from subtracting the interfacial potential drops (double-layer formation) from the applied voltage (e.g., 5 V). For $\mu_{Ru^+} = 2.5 \times 10^{-8}$ m^2 V^{-1} s^{-1} (assessed from radius of the rubrene molecule and the viscosity of the solvent $= 4.55 \times 10^{-4}$ N s m^{-2} [42]), dielectric permittivity of the solvent $\epsilon = 7.2$,[42] interelectrode distance $d = 64\ \mu$m, and assessed effective voltage drop $U_{eff} = 1$ V, a current density of only $j_{sclc} = 0.7$ nA cm^{-2} is obtained. Assuming that convection contribution in the first approximation can be treated in terms of enhancing the effective (i.e., now mainly hydrodynamic) ionic mobility μ, the latter one would have to be as high as 0.037 m^2 V^{-1} s^{-1} in order to account for the experimentally observed current density (1 mA cm^{-2} for $U = 5$ V, cf. curve 7, Figure 3a). Since the velocity v under the influence of an electric field is given by $v = \mu E$, for this situation the fluid velocity of nearly 600 m s^{-1} would result, which is completely unrealistic and is in contrast to the fact that the experimentally observed velocity does not exceed a few mm s^{-1}. Thus, the concept of unipolar charge injection can explain neither the currents observed in this work nor the ones reported earlier.[22,23,26]

The reported current can be understood only if the solution has an appropriate conductivity, assured by the presence of background electrolyte. On the other hand, the existence of appropriate uncompensated space charge in the bulk solution is possible if the concentration of supporting electrolyte is low enough. Thus, for the practical functioning of the electrochemiluminescent convective cell there exists an *optimum* concentration of background electrolyte that was found to be of the order $10^{-6}-10^{-5}$ mol dm^{-3}.

On the basis of above considerations showing the role of supporting electrolyte, one may understand the course of the current−voltage characteristics of the system, presented in Figure 3, in the following way. The interfacial electron-transfer processes of rubrene (eqs 2 and 3) are fast and reversible. Thus, the electric current is controlled both by the conductivity of the solution and by the fraction of surface of the electrodes, at which the electric double layers of the required value of $\Delta\varphi_{dl}$ have been formed. The electrode areas where both these conditions are fulfilled manifest themselves as luminescent regions. The extent of luminescence from the peripheral toward the central areas of electrodes rises as a function of time (also at a constant voltage), reflecting in this way the stepwise inflow of missing supporting electrolyte from the surrounding solution. Accordingly, the current rises as a function of time, and this is the source of hysteresis observed on subsequently recorded $I-U$ curves.

For estimating the driving force for convection in our experimental conditions, consider that according to Poisson's equation the excess space charge density q_{ex} in the solution is related to the divergence of the electric field, along the x coordinate oriented perpendicularly to electrode surfaces, by $q_{ex} = \epsilon\epsilon_0(dE_x/dx)$. For the typical conditions of our experiments, the absolute value of the electric field in the bulk solution between the electrodes is of the order of $E_x = 100$ V cm^{-1}. If the space charge injection decreases the field at the emitter

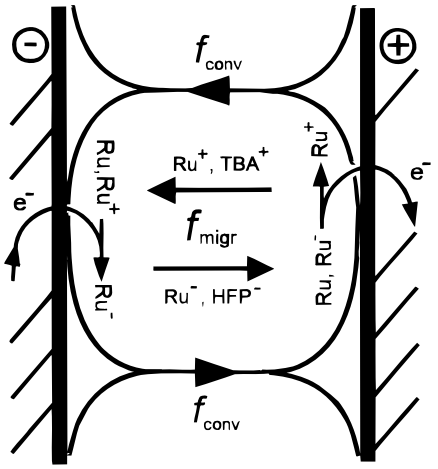

Figure 6. Schematic picture of electrochemical processes occurring in a single convective roll of the EHD thin-layer cell. Electrode reactions of rubrene at the interfaces are accompanied with convection (f_{conv}) and migration (f_{migr}) of ions of rubrene and the background electrolyte. For simplification, diffusion fluxes were not indicated.

electrode to zero, the corresponding (mean) divergence of the field with respect to the center of the cell is $dE_x/dx \simeq 2 \times 10^4$ V cm^{-2}. The corresponding mean excess space charge density in the bulk solution is then equal to 13 nC cm^{-3}. Thus, the mean driving force for convection is $F_x = q_{ex}E_x = 1.3 \times 10^{-4}$ N cm^{-3}. It is noteworthy that this excess space charge density is smaller by about 5 orders of magnitude than the total density of ions in the bulk solution. This means that−aside from above considerations on the convective driving force−the electrochemiluminescent thin-layer system can be considered a classical two-electrode electrochemical cell, for which (a) outside the regions of the electrical double layers electroneutrality prevails and (b) the rates of anodic and cathodic interfacial charge-transfer processes are practically identical.

During operation of the electrochemiluminescence cell the ions of background electrolyte as well as the rubrene molecules and ions are involved in transport processes.

The detailed transport mechanism comprising convection, migration, and diffusion is complex. Only a qualitative picture will be given in the following. The basic consideration is that locally different transport processes prevail. In the convective flows that form the EHD cells the convective transport dominates. In the interior regions of the EHD cells migration dominates (Figure 6). The corresponding fluxes of rubrene ions are expressed by the following formulas:

$$f_{conv}(Ru^+,Ru^-) = (\mu_H E)C_{Ru^+,Ru^-} = v_{conv}(U_{eff})C_{Ru^+,Ru^-} \quad (8a)$$

$$f_{migr}(Ru^+,Ru^-) = (\mu_{Ru^+,Ru^-}E)C_{Ru^+,Ru^-} = v_{migr}(U_{eff})C_{Ru^+,Ru^-} \quad (8b)$$

where the voltage-dependent velocities of convection v_{conv} and migration v_{migr} are the products of the electric field intensity E and (i) hydrodynamical mobility of the solvent, defined as $\mu_h = v_{conv}/E$, and (ii) the migration mobility of rubrene ions μ_{Ru^+,Ru^-}, respectively.

The morphology of the luminescencent pattern does not depend on the polarization and the type of electrode (metal, ITO semiconductor). This indicates that the electrochemiluminescence originates from the recombination reaction 4 occurring in the solution.

The shape of luminescent patterns is determined by the distribution of fluxes of rubrene ions and by the locations of

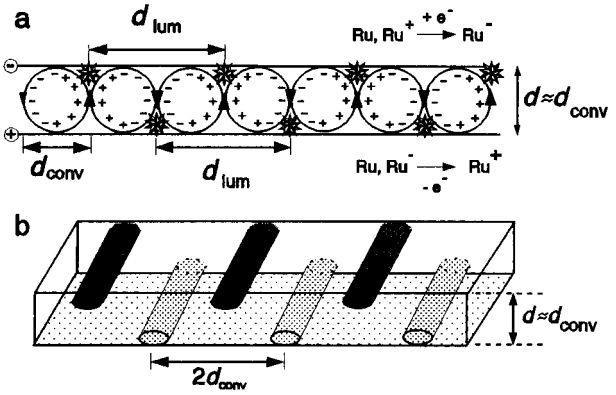

Figure 7. Mechanism for generation of linear patterns of luminescence exhibiting the spatial period (d_{lum}) doubling the interelectrode distance (d): (a) visible luminescence (asterisks) occurs where the convective streams carrying rubrene ions formed at one electrode approach the other electrode (cf. Figure 6); (b) three-dimensional distribution of cathodic−anodic luminescence; the traces in the cathodic and anodic layers are mutually shifted for the value comparable with the interelectrode distance d in the plane parallel to the electrodes.

the electrochemical reactions (cf. Figures 6 and 7). The emission of light occurs mainly in regions where the electrode surface is hit by the convective flows rich in rubrene ions, arriving from the opposite electrode. There the product of concentrations of these ions (e.g., Ru^+ at the cathode) and ions of the opposite sign formed electrochemically (Ru^-) is highest. Thus, if the cross section of a single convective flow is approximately circular or quadratic,[3,9,10] the distance between neighboring luminescence traces at one electrode is expected to be twice the interelectrode distance (Figure 7).

For an explanation of the asymmetric distribution of luminescence across the interelectrode distance, it is important to realize that the mobilities of the ions Ru^+, TBA^+, and Ru^- are approximately equal, $\mu \simeq 2.7 \times 10^{-8}$ m^2 V^{-1} s^{-1}. However, the mobility of HFP^- is $\mu_{HFP^-} \simeq 1.2 \times 10^{-7}$ m^2 V^{-1} s^{-1}, i.e., larger by more than a factor of 4. As a consequence, the extent of migrational transfers of Ru^- from the cathode to the anode and of Ru^+ in the opposite direction will be different. The places of recombination reaction will thus not be distributed symmetrically in the interelectrode space. This explains the asymmetry of the cathodic and anodic luminescence intensity, despite the symmetry of the charge-transfer processes at both electrodes. The detailed explanation of the luminescence distribution needs a knowledge of space distribution of the velocities of convective flows.

Finally, it should be noted again that in all the experiments described above the thin-layer cell could be oriented only vertically. In this geometry a contribution of thermal convection, setting in at any temperature gradient resulting from the Joule heating of the electrolyte, cannot be excluded. However, a comparison of our experiments with results of other researchers shows that all types of structures reported by Jaguiro et al.[26,29,40] for horizontally oriented electrodes were found also in our experiments. Thus, it may be concluded that the convection patterns described are indeed electrohydrodynamic phenomena.

5. Summary

An experimental setup is described that allows to study electrohydrodynamic convection in a thin-layer cell with precisely and smoothly adjustable interelectrode distance. Experiments show that with a thoroughly purified solution of rubrene in 1,2-dimethoxyethane neither significant current nor luminescence is observed until small amounts of supporting electrolyte are added. Convection and migration of rubrene ions proceed in a largely electroneutral environment. The counterions originate from the background electrolyte. In the electric field, only the very small uncompensated space charge leads to a driving force for electrohydrodynamic convection. A *bipolar* mechanism for the formation of chemiluminescence patterns operates which, contrary to previous *unipolar* models, involves electrochemical creation of both rubrene anions and cations followed by transport through the solution and subsequent recombination in regions near the respective opposing electrodes. This mechanism is able to qualitatively account for all the observed phenomena, such as the formation of luminescence patterns (with differing intensities) in the regions of both anode and cathode, as well as their geometric features.

Acknowledgment. M.O. gratefully acknowledges a fellowship from the A. v. Humboldt Foundation.

References and Notes

(1) Nicolis, G.; Prigogine, I. *Self-Organization in Nonequilbrium Systems*; Wiley: New York, 1977.
(2) Ebeling, W.; Feistel, R. *Physik der Selbstorganization und Evolution*; Akademie-Vlg.: Berlin, 1982.
(3) Bergé, P.; Pomeau Y.; Vidal, C. *Order Within Chaos. Towards a Deterministic Approach to Turbulence*; Wiley-Hermann: Paris, 1984 and references therein.
(4) Orlik, M. *Oscillating Reactions. Order and Chaos*; WNT: Warsaw, 1996 (in Polish).
(5) Bénard, H. *Rev. Gen. Sci. Pure Appl.* **1900**, *12*, 1261, 1309.
(6) Bergé, P. Rayleigh-Bénard Convection in High Prandtl Number Fluid. In Haken, H., Ed. *Chaos and Order in Nature*; Proc. Int. Symp. Synergetics; Springer: Berlin, 1984; pp 14, 1981.
(7) Lord Rayleigh *Philos. Mag.* **1916**, *32*, 529.
(8) Chandrasekhar, S. *Hydrodynamic and Hydromagnetic Stability*; Oxford University Press: New York, 1961.
(9) Küppers, G. Selbstorganisation: Selektion durch Schliessung. In *Chaos und Ordnung. Formen der Selbstorganisation in Natur und Gesellschaft*; Küppers, G., Ed.; Reclam: Stuttgart, 1996.
(10) Kessler, R. *J. Fluid Mech.* **1987**, *174*, 357.
(11) Baranowski, B.; Kawczynski, A. L. *Rocz. Chem. Ann. Soc. Chim. Polonorum* **1970**, *44*, 2447.
(12) Baranowski, B.; Kawczynski, A. L. *Electrochim. Acta* **1972**, *17*, 695.
(13) Baranowski, B. *J. Non-Equilib. Thermodyn.* **1980**, *5*, 67.
(14) Baranowski, B. *Nova Acta Leopold.* **1989**, *60*, 91.
(15) Winkler, I.; Plevan, I.; Nechiporuk, V. *Electrochim. Acta* **1996**, *41*, 2743.
(16) Schneider, J. M.; Watson, P. K. *Phys. Fluids* **1970**, *13*, 1948.
(17) Watson, P. K.; Schneider, J. M.; Till, H. R. *Phys. Fluids* **1970**, *13*, 1955.
(18) Felici, N.; Lacroix, J. C. *J. Electrostat.* **1978**, *5*, 135.
(19) Atten, P.; Lacroix, J. C. *J. Electrostat.* **1978**, *5*, 439.
(20) Lacroix, J. C.; Atten, P. *J. Electrostat.* **1978**, *5*, 453.
(21) Köstlin, H.; Schaper, H. *Phys. Lett.* **1980**, *76A*, 455.
(22) Schaper, H.; Köstlin, H.; Schnedler, E. *J. Electrochem. Soc.* **1982**, *129*, 1289.
(23) Schaper, H.; Schnedler, E. *J. Phys. Chem.* **1982**, *86*, 4380.
(24) Schaper, H.; Schnedler, E. *J. Electroanal. Chem.* **1982**, *137*, 39.
(25) Schaper, H. *J. Electroanal. Chem.* **1981**, *129*, 335.
(26) Jaguiro, P. *Proc. SPIE−Int. Soc. Opt. Eng.* **1996**, *2729*, 131−8.
(27) Jaguiro, P.; Smirnov, A. *Proc. SPIE−Int. Soc. Opt. Eng.* **1995**, *2373*, 401−8.
(28) Jaguiro, P. V.; Zhivnov, V. A. *Izv. Akad. Nauk SSSR, Ser. Phys.* **1987**, *51*, 591 (in Russian).
(29) Solodkov, V. T.; Jaguiro, P. V.; Zhirnov, V. A. *Elektron. Obrab. Mater.* **1990**, *152*, 34 (in Russian).
(30) Felici, N. *Rev. Gen. Electr.* **1969**, *78*, 717.
(31) Felici, N. *Direct Current* **1972**, *2*, 147.
(32) Williams, R. *J. Chem. Phys.* **1963**, *39*, 384.
(33) *Cellular Structures in Instabilities*; Lecture Notes in Physics 210; Wesfreid, J. E., Zaleski, S., Eds.; Springer: Berlin, 1984.
(34) Lowe, M.; Gollub, J. P.; Lubensky, T. C. *Phys. Rev. Lett.* **1983**, *51*, 786.
(35) Zaslavskii, G. M.; Sagdeev, R. E. *Introduction to a nonlinear physics. From pendulum to turbulence and chaos*; Nauka: Moscow, 1988 (in Russian).

(36) Helfrisch, W. *J. Chem. Phys*. **1969**, *51*, 4092.
(37) Takahashi, A.; Aikawa, Y.; Toyoshima Y.; Sukigara, M. *J. Phys. Chem*. **1979**, *83*, 2854.
(38) Bard, A. L.; Faulkner, L. R. *Electrochemical Methods*; Wiley: New York, 1980.
(39) Kapturkiewicz, A. *J. Electroanal. Chem*. **1994**, *372*, 101.
(40) Jaguiro, P. Private communication.
(41) *CRC Handbook of Chemistry and Physics*, 64th ed.; CRC Press: Boca Raton, FL, 1983−1984.
(42) Riddick, J. A., Bunger, W. B., Sakano, T. K., Eds. *Techniques of Chemistry; Vol. II (Organic Solvents)*, 4th ed.; Wiley: New York, 1986; p 296.